Cell Reports, Volume *22*

Supplemental Information

A Pixel-Encoder Retinal Ganglion Cell with Spatially Offset Excitatory and Inhibitory Receptive Fields

Keith P. Johnson, Lei Zhao, and Daniel Kerschensteiner

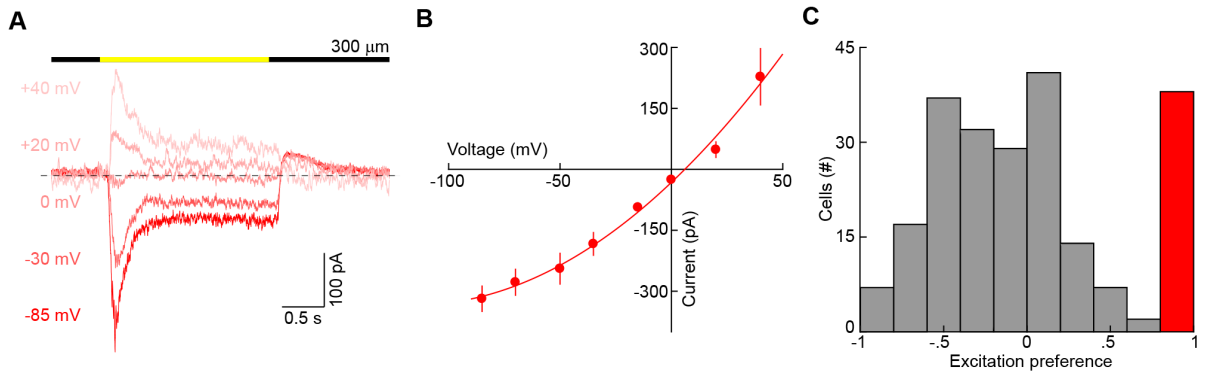

Figure S1. Current-voltage relationship of synaptic inputs to Pix_{ON}-RGCs elicited by small stimuli (related to Figure 1)

(A) Currents evoked by presentation of a 300 µm circle (2 s ON, 2 s OFF, background: 1500 R*/rod/s) at different holding potentials. (B) Summary peak current versus voltage curve (n = 5). Line is fit of data by a second order polynomial. (C) Histogram showing excitation preferences of all cells (gray) in Grik4-Cre:Ai9 for which both excitatory and inhibitory currents were recorded during presentation of a 300-µm circle. The histogram of Pix_{ON}-RGCs' excitation preference is overlaid in red.

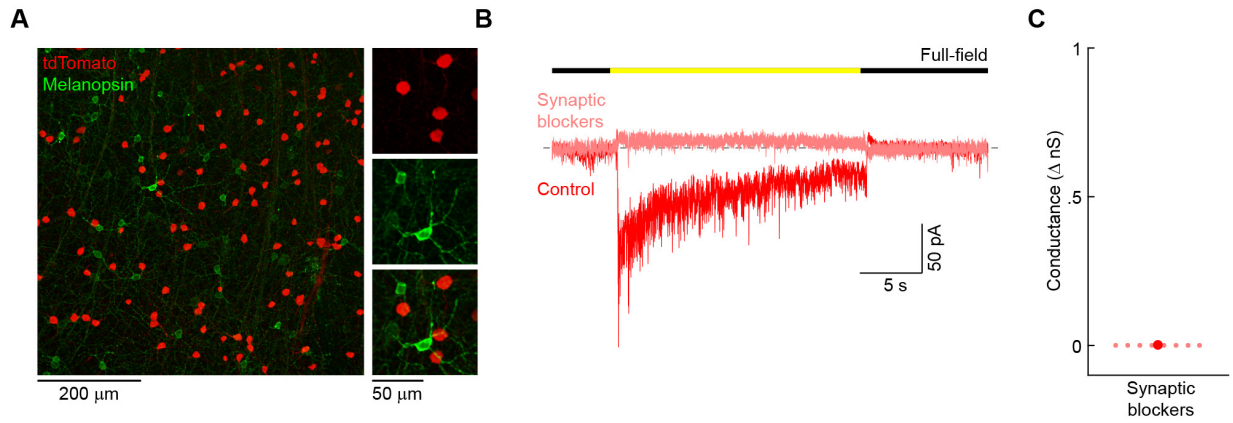

Figure S2. Pix$_{ON}$-RGCs do not stain for melanopsin and are not intrinsically photosensitive (related to Figure 1)

(A) Melanopsin staining in a Grik4-Cre:Ai9 retina. (B) Representative EPSCs of a Pix$_{ON}$-RGC to full-field light stimulation in control conditions (red) and under blockade of synaptic inputs to Pix$_{ON}$-RGCs (light red). Dashed line shows baseline in the absence of stimulus. (C) Summary of excitatory conductance evoked by full-field light stimulation in the presence of synaptic blockers (n = 8). Stimuli were presented at ~1000 R* (~2 * 10^{11} photons / cm^2 / s) and ~10^7 R* (~2 * 10^{15} photons / cm^2 / s).

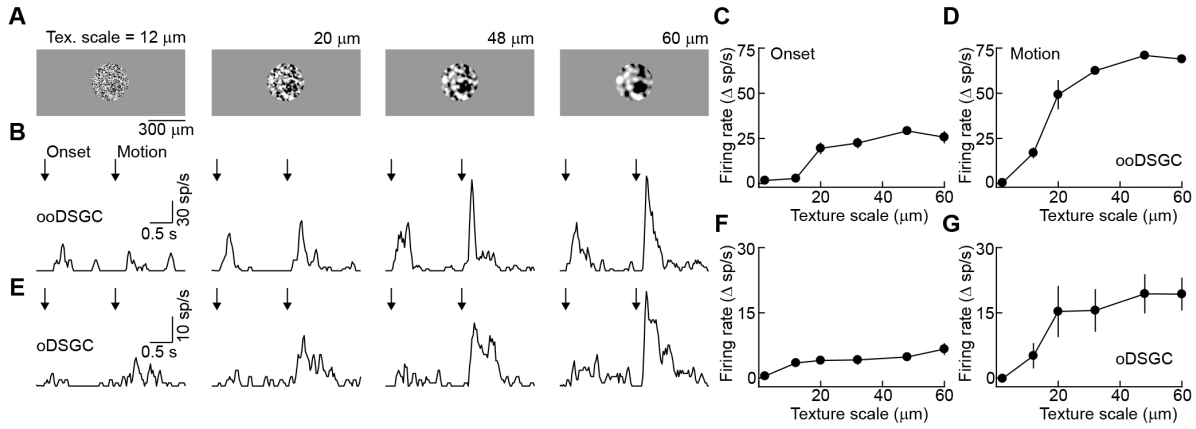

Figure S3. Responses of direction-selective ganglion cells in Grik4-Cre:Ai9 to texture stimuli (related to Figure 2)

(A) Representative texture stimuli of different spatial scales masked in a 300 μm circle. Textures appeared from a grey background (onset) and were then translated 33 μm in either the dorsal, ventral, nasal, or temporal direction (motion). Textured regions had the same mean luminance as the background. (B) Representative spike responses of an ON-OFF DSGC (ooDSGC) to presentation of textures of the spatial scales shown in (A). (C, D) Summary of ON-OFF DSGC spike responses to the onset (C, n = 4) and motion (D, n = 4) of texture stimuli of different spatial scales. ON-OFF DSGCs exhibited directional preference during texture motion. Firing rates shown are for motion in the preferred direction. (E) Representative spike responses of an ON DSGC (oDSGC) to presentation of textures of the spatial scales shown in (A). (F, G) Summary of ON DSGC spike responses to the onset (F, n = 4) and motion (G, n = 4) of texture stimuli of different spatial scales. ON DSGC exhibited directional preference during texture motion. Firing rates shown are for motion in preferred direction.

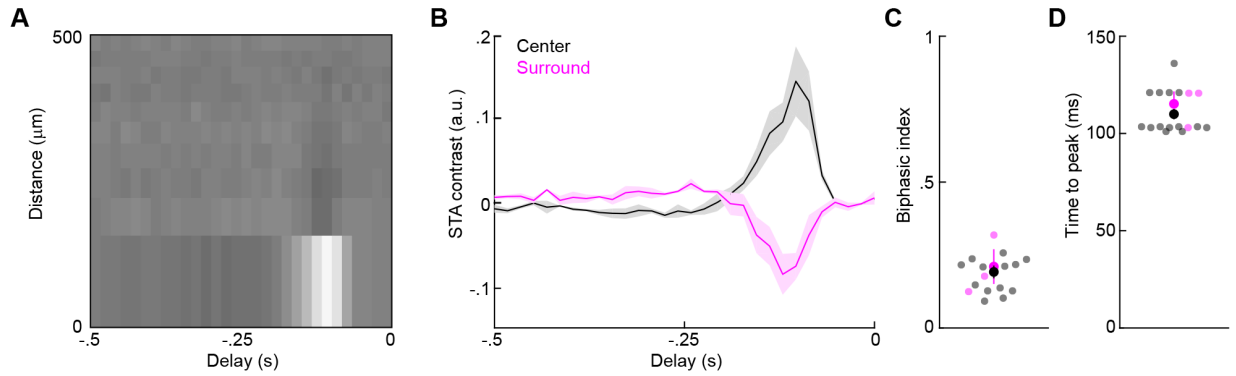

Figure S4. Spatiotemporal receptive fields of Pix_{ON}-RGCs (related to Figures 1, 2 and 3)

(A) Representative spatiotemporal receptive field map of a Pix_{ON}-RGC measured from its spike response to a circular white noise stimulus with rings of constant area. (B) Spike-triggered average (STA) responses of the center (300 μm circle) and surrounding rings (n = 3). An additional 11 cells were recorded in which the white noise stimulus was only presented within the center 300 μm circle. Lines (shaded areas) indicate the mean (± SEM) temporal kernels of the center (black) and surround (magenta) regions. (C) Summary of STA biphasic indices (STA peak/|STA trough|) (n = 14 center, n = 3 surround). (D) Summary of times to the STA peak (n = 14 center, n = 3 surround).

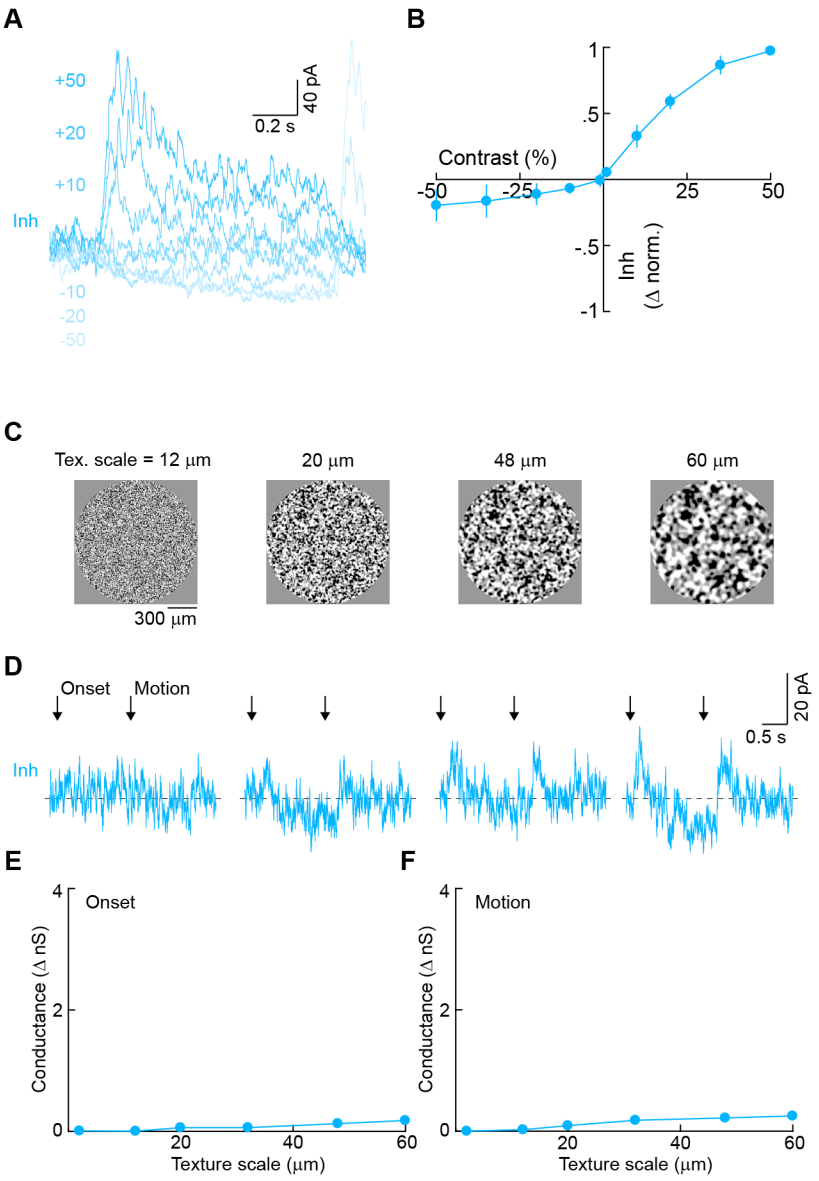

Figure S5. Contrast response function and texture responses of inhibition to Pix_{ON}-RGCs (related to Figure 2)

(A) Representative IPSC responses to contrast steps presented in a 1200-μm circle centered on the soma of the recorded cell. Dashed line shows baseline in the absence of stimulus. (B) Contrast response function of normalized inhibitory conductance (B, n = 4). (C) Texture stimulus as described in Figures 3 and S3, but here textures are masked in a 1200-μm circle. (D) Representative inhibitory responses of a Pix_{ON}-RGC to the presentation of textures of the spatial scales shown in (C). (E, F) Summary of Inhibitory responses to the onset (E, n = 3) and motion (F, n = 3) of texture stimuli of different spatial scales.

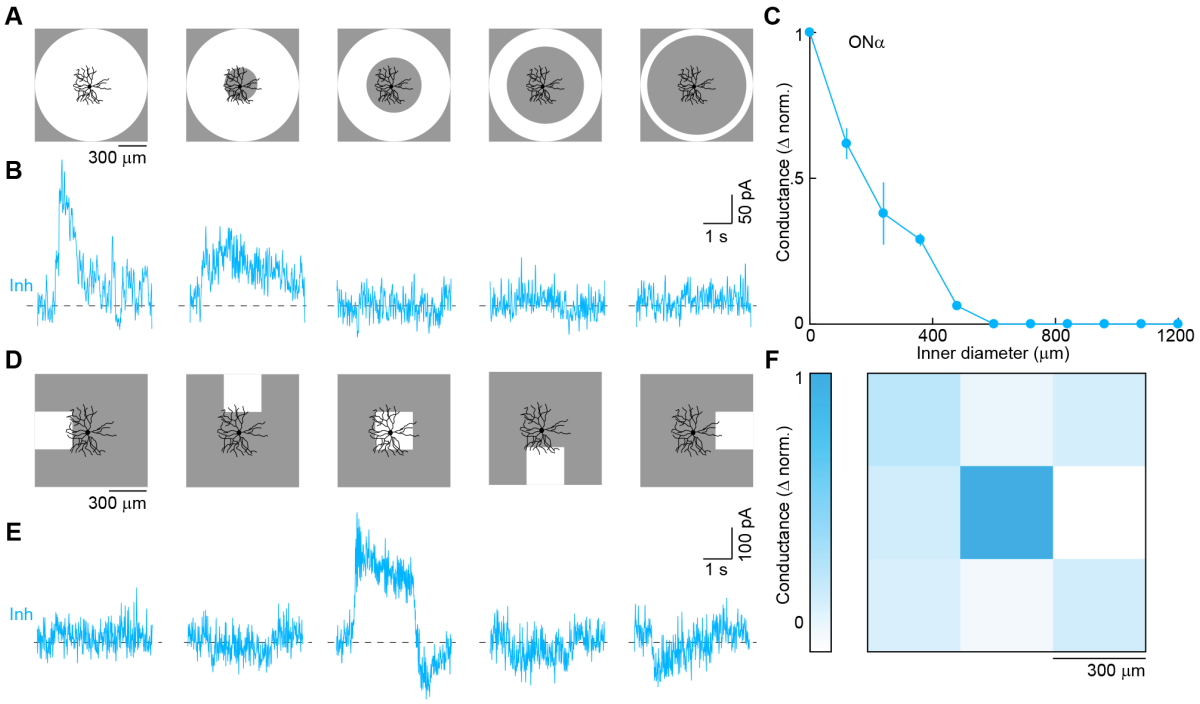

Figure S6. Inhibitory receptive fields of ONα-RGCs (related to Figure 5)

(A) Annuli of constant outer diameter (1200 µm) and varying inner diameter were presented as 100% contrast steps (2 s ON) from a grey background (1500 R*/rod/s). (B) Representative IPSCs in an ONα-RGC in response to annuli shown in (A). (C) Normalized inhibitory conductance versus annulus inner diameter (n = 3). (D) The display was divided into a 3 x 3 gird of 300 µm x 300 µm squares and centered on the soma of the recorded cell. Between stimulus presentations all squares had the same luminance (1500 R*/rod/s). During stimulus presentation, one of the nine squares increased in luminance (100% contrast, 2 s ON). (E) Representative IPSCs in an ONα-RGC in response to appearance of squares in the positions shown in (D). (F) Map of the normalized inhibitory conductance evoked by the appearance of a square at each position (n = 2).

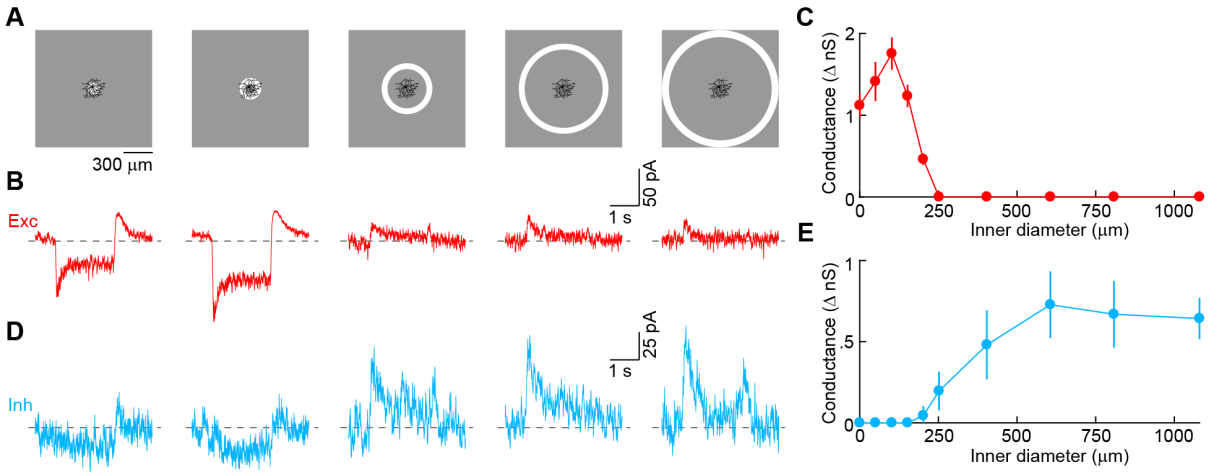

Figure S7. Spatial separation of excitatory and inhibitory receptive fields of Pix$_{ON}$-RGCs (related to Figure 5)

(A) Annuli of constant width (60 µm) and varying inner diameters were square-wave modulated (2 s ON, 2 s OFF, background: 1500 R*/rod/s). (B, D) Representative excitatory (B, red) and inhibitory (D, cyan) currents evoked by annuli shown in (A). Dashed lines show baselines in the absence of stimulus. (C) Excitatory conductance (inward only) versus annulus inner diameter (n = 4). (E) Inhibitory conductance (outward only) versus annulus inner diameter (n = 8).